

Direct electrical stimulation impacts on neuromuscular junction morphology on both stimulated and unstimulated contralateral soleus

Young il Lee^{1,2} , Nicola Cacciani³, Ya Wen³, Xiang Zhang⁴, Yvette Hedström³, Wesley Thompson^{1,5} & Lars Larsson^{3,6,7*} 

¹Department of Biology, Texas A&M University, College Station, TX, USA; ²Department of Pharmacology & Therapeutics, College of Medicine, University of Florida Myology Institute, University of Florida, Gainesville, FL, USA; ³Department of Physiology and Pharmacology, Basic and Clinical Muscle Biology Group, Karolinska Institutet, Stockholm, Sweden; ⁴Department of Molecular Medicine and Surgery, Karolinska Institutet, Stockholm, Sweden; ⁵Section of Molecular Cell and Developmental Biology, The University of Texas, Austin, TX, USA; ⁶Department of Clinical Neuroscience, Section of Clinical Neurophysiology, Karolinska Institutet, Stockholm, Sweden; ⁷Viron Molecular Medicine Institute, Boston, MA, USA

Abstract

Background There is increasing evidence of crosstalk between organs. The neuromuscular junction (NMJ) is a peripheral chemical synapse whose function and morphology are sensitive to acetylcholine (ACh) release and muscle depolarization. In an attempt to improve our understanding of NMJ plasticity and muscle crosstalk, the effects of unilateral direct electrical stimulation of a hindlimb muscle on the NMJ were investigated in rats exposed long-term post-synaptic neuromuscular blockade.

Methods Sprague Dawley rats were subjected to post-synaptic blockade of neuromuscular transmission by systemic administration of α -cobrototoxin and mechanically ventilated for up to 8 days and compared with untreated sham operated controls and animals exposed to unilateral chronic electrical stimulation 12 h/day for 5 or 8 days.

Results NMJs produced axonal and glial sprouts (growth of processes that extend beyond the confines of the synapse defined by high-density aggregates of acetylcholine receptors [AChRs]) in response to post-synaptic neuromuscular blockade, but less than reported after peripheral denervation or pre-synaptic blockade. Direct electrical soleus muscle stimulation reduced the terminal Schwann cell (tSC) and axonal sprouting in both stimulated and non-stimulated contralateral soleus. Eight days chronic stimulation reduced ($P < 0.001$) the number of tSC sprouts on stimulated and non-stimulated soleus from 6.7 ± 0.5 and 6.9 ± 0.5 sprouts per NMJ, respectively, compared with 10.3 ± 0.9 tSC per NMJ ($P < 0.001$) in non-stimulated soleus from rats immobilized for 8 days. A similar reduction of axonal sprouts ($P < 0.001$) was observed in stimulated and non-stimulated contralateral soleus in response to chronic electrical stimulation. RNAseq-based gene expression analyses confirmed a restoring effect on both stimulated and unstimulated contralateral muscle. The cross-over effect was paralleled by increased cytokine/chemokine levels in stimulated and contralateral unstimulated muscle as well as in plasma.

Conclusions Motor axon terminals and terminal Schwann cells at NMJs of rats subjected to post-synaptic neuromuscular blockade exhibited sprouting responses. These axonal and glial responses were likely dampened by a muscle-derived myokines released in an activity-dependent manner with both local and systemic effects.

Keywords Neuromuscular junction; Post-synaptic neuromuscular blockade; Chronic electrical stimulation; Soleus muscle; Crossover effect; Terminal sprouting

Received: 29 September 2022; Revised: 6 March 2023; Accepted: 15 March 2023

*Correspondence to: Lars Larsson, Department of Physiology and Pharmacology, Karolinska Institutet, SE-171 77 Stockholm, Sweden. Email: lars.larsson@ki.se

Introduction

The neuromuscular junction (NMJ) is the cholinergic synapse that forms at the site of contact between a motor axon terminal and a skeletal muscle fibre. Examination of this peripheral chemical synapse, in both health and disease, has informed our fundamental understanding of chemical synapses in both the peripheral and central nervous systems. Although, the morphology of a mature rodent NMJ and its cellular components are stable, changes are observed when subjected to insults including neuromuscular diseases, aging and interruption of synaptic transmission, either through physical or pharmacological means.¹ One common response is the production of axonal sprouts which allows the functional re-innervation of silenced muscle fibres. Processes produced by terminal Schwann cells (tSC) both promote and guide the axonal sprouts away from intact synapses when synaptic transmission at NMJs is interrupted.^{2,3} The NMJ is, thus, a dynamic structure that can produce a compensatory response when its ability to elicit a functional response from the postsynaptic muscle fibre is compromised.

The ability of postsynaptic acetylcholine receptor (AChR) blockade by local intramuscular injection of one antagonist, α -bungarotoxin to illicit a sprouting response from motor axons, as well as the reduced sprouting response with direct electrical muscle stimulation indicate that the stimulus to muscle sprouting is derived from the inactive target muscle fibres.⁴ Observations suggest this stimulus for terminal sprouting is a short-range cue(s) that influences the synapse that resides on the silenced fibre and those of immediate neighbouring fibres.⁵ Several factors have been implicated in production of sprouting response, however, the identity of such 'sprouting factor' remains unresolved.

This study was undertaken to study the impact of long-term, systemic pharmacological denervation by post-synaptic blockade of neuromuscular transmission on the NMJ with and without direct electrical muscle stimulation. The severe muscle wasting observed in paralysed/immobilized intensive care unit (ICU) patients has a significant negative impact on recovery, post-ICU rehabilitation and affect patient quality of life many years after hospital discharge.⁶ Thus, electrical stimulation not requiring active participation from a mechanically ventilated, deeply sedated or pharmacologically paralysed ICU patients offers an attractive intervention aiming at mitigating the muscle wasting associated with modern critical care.⁷

Methods

Animals and experimental intensive care unit model

A total of 20 female 280–350 g Sprague Dawley rats were examined. Four 0 day sham operated control rats were included

together with experimental rats exposed to deep sedation with isoflurane, mechanical ventilation and pharmacological paralysis post-synaptically by α -cobrotoxin for 5 ($n = 4$) and 8 ($n = 4$) days. Rats exposed to unilateral supramaximal direct stimulation for 5 ($n = 4$) and 8 ($n = 4$) days were also included. All ventilated animals were maintained in fluid and nutritional balance throughout the duration of the experimental procedures and monitored extensively 24 h/day.

Electrical stimulation, gene, and protein analyses.

Stimulation electrodes were implanted in the right soleus and stimulated 12 h/day (20 Hz for 10 s every 20 s). After animals were euthanized, soleus muscles were dissected and fixed in 4% phosphate-buffered paraformaldehyde. The NMJ and its components were fluorescently labelled and analysed. RNAseq-based transcriptomic and proteomic analyses were performed in sham-operated control rats, 8 day pharmacologically denervated, 8 day pharmacologically denervated and electrically stimulated and unstimulated contralateral soleus muscles. Soleus and plasma proteomic analyses were performed using the Olink® Target 96 Mouse Exploratory panel (Olink Proteomics AB, Uppsala, Sweden).

For details related to ethical permission, experimental setup, chronic electrical stimulation, NMJ preparation, RNAseq, proteomics, and statistics, see supporting information.

Results

Morphological changes were observed at NMJs in response to long-term post-synaptic blockade of neuromuscular transmission, that is, a pharmacological denervation with an intact α -motoneuron axon terminal still apposed the postsynaptic AChR aggregates of each muscle fibre.

Postsynaptic acetylcholine receptor aggregates and muscle fibre size

Animals were paralysed by the short neurotoxin α -cobrotoxin to ensure complete post-synaptic blockade of neuromuscular transmission. The neurotoxin was given as an initial bolus dose and followed by continuous infusion, as new AChRs are synthesized and the α -cobrotoxin blockade is not irreversible.⁸ The long neurotoxin α -bungarotoxin binds more strongly than α -cobrotoxin and on distinct portions of AChRs to form a quasi-irreversible binding to the receptor. AChRs can accordingly be visualized by the α -bungarotoxin despite previous α -cobrotoxin-mediated blockade of neuromuscular synaptic transmission. The overall appearance of postsynaptic AChR aggregates of immobilized and ventilated animals did not qualitatively differ from those of control animals

(Figure 1). However, long-term immobilization by neuromuscular blockade appears to decrease the counts of discrete AChR-rich segments (or islands) (Figure 1B; control: 5.3 ± 0.5 ; 5 days immobilized: 3.2 ± 0.3 ; 8 days immobilized:

3.2 ± 0.4 ; $P < 0.001$). Although, the mechanism for such change is unclear, it may be related to disuse atrophy of the muscle fibres of paralysed animals undergo because endplate size has been reported change with the size of muscle fibres.⁹

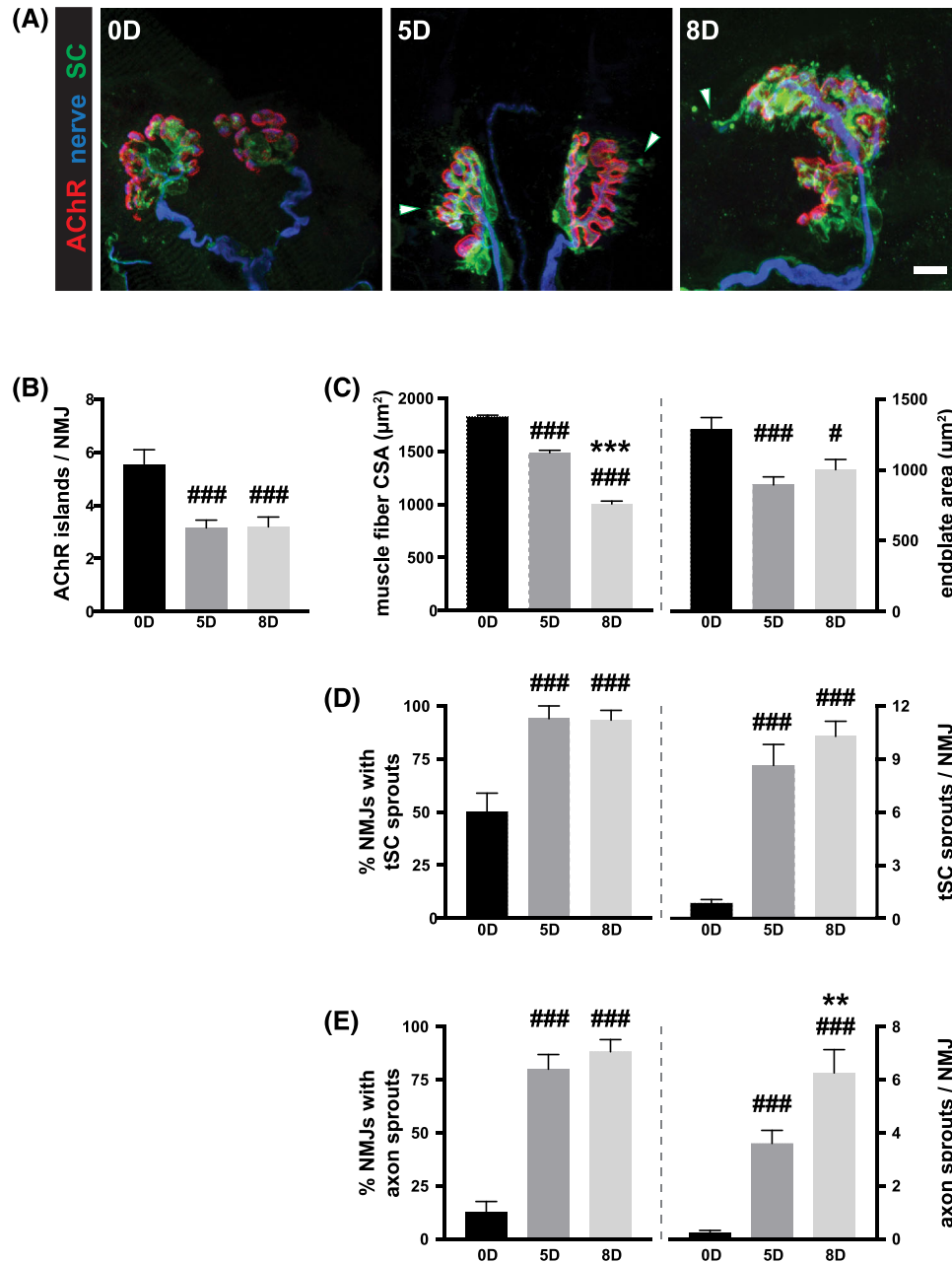


Figure 1 Prolonged silencing of rat neuromuscular junctions via post-synaptic AChR blockade leads to alterations of synaptic components. (A) In every condition, there exists a good registration between the postsynaptic AChR aggregates (red) and the terminal branches of the innervating motor axon (blue) while the terminal Schwann cells (tSCs; green) provide good coverage of the synapse. Scale bar = 10 μm. (B–D) Postsynaptically, there is a noticeable decrease in the number of discrete AChR-rich islands at soleus NMJs of paralysed rats (B). This likely is a consequence of disuse atrophy of muscle fibres and the accompanying reduction in the synaptic area (C). Glial and neuronal component of NMJs show a sprouting response (D, E). For both the tSCs (D) and motor axon terminals (E), the fraction of NMJs with sprouts and the number of sprouts per synapse show a marked increase after immobilization. One-way ANOVA, Tukey post-hoc analysis: ### $P < 0.001$, # $P < 0.05$ vs. non-immobilized control cohort *** $P < 0.001$, ** $P < 0.01$; 8- vs. 5-days immobilized experimental cohorts.

Indeed, the cross-sectional area of isolated single fibres measured at a fixed sarcomere length decreased progressively from $1830 \pm 20 \mu\text{m}^2$ ($n = 4$ animals, 52 isolated fibres) in control animals to $1490 \pm 30 \mu\text{m}^2$ ($n = 4$ animals, 48 isolated fibres) and $1010 \pm 30 \mu\text{m}^2$ ($n = 4$ animals, 56 isolated fibres) after 5 and 8 days of ICU condition ($P < 0.001$). (Figure 1C). Indeed, the endplates from animals subjected to 5 and 8 days of ICU condition show a corresponding decrease in size compared with those that reside on muscle fibres of control rats (Figure 1C; control: $1290 \pm 80 \mu\text{m}^2$, $n = 47$ from 4 animals; 5 days immobilized: $900 \pm 60 \mu\text{m}^2$, $n = 53$ from 3 animals; 8 days immobilized: $1000 \pm 70 \mu\text{m}^2$, $n = 49$ from 3 animals; $P < 0.05$ – 0.001).

Moreover, despite reports of reduced muscle excitability in response to long-term blockade and immobilization in clinical studies in ICU patients with CIM,¹⁰ voltage-gated Na⁺ channels remained concentrated at the postsynaptic muscle membrane, as well as at the nodes of Ranvier along the pre-terminal segments of the motor axons (Figure S1). The molecular assembly of proteins that renders the muscle fibres sensitive to contractions in response to α -motoneuron discharge, therefore, appears unperturbed in our rodent model of long-term pharmacological denervation.

Terminal sprouting

There were no overall rearrangements of the existing synaptic structure in response to the pharmacological denervation. Each muscle fibre remains innervated by a single axon (Figure S2A) and the degree of its arborisation (determined by the number of branch points of axon terminals within the endplates) remained largely unchanged, regardless of the duration of pharmacological denervation (Figure S2B). The complement of tSCs also remained relatively constant (Figure S2C). The glial and neuronal components of NMJs, nonetheless, underwent subtle, but specific and quantifiable changes. The most prominent morphological adaptations observed at the NMJs were the production of sprouts by both motor axon terminals (Figure 1D) and tSCs (Figure 1E).

Although tSCs at approximately half ($50.0 \pm 9.0\%$) of the NMJs of normal animals presented with processes that extended short distances beyond the confines of the pre-/post-synaptic apposition, the frequency with which such sprouts were observed increased progressively with increasing duration of post-synaptic blockade of neuromuscular transmission. By 5 days of immobilization, virtually, all NMJs showed a glial sprouting response that was maintained through 8 days of immobilization (Figure 1D; 5 days immobilization: $97.1 \pm 2.9\%$ and 8 days immobilization $93.3 \pm 4.6\%$; $P < 0.05$, one-way ANOVA with Tukey post hoc vs. control: $P < 0.001$ for 5 and 8 days immobilized). Motor axon terminals, similarly, responded with an increased sprouting behaviour (Figure 1E): $76.9 \pm 5.9\%$ and $88.2 \pm 5.6\%$, respectively,

compared with only a small fraction of NMJs that produced axonal sprouts in control animals ($12.8 \pm 4.9\%$; $P < 0.05$, one-way ANOVA with Tukey post hoc vs. control: $P < 0.001$ for 5 and 8 days immobilized animals). Despite the marked increase in the fraction of NMJs that showed sprouting response with regard to both motor axon and tSCs, it is worth noting that the frequency with which one encounters axonal sprouts (i) appears markedly less than with tSC sprouts at all time-points examined and, (ii) despite continued increase until the experimental endpoint, did not reach tSC levels.

Concurrently, the numbers of these sprouts increased progressively with increasing duration of neuromuscular blockade. On average control NMJ produces <1 (0.9 ± 0.2) glial sprout (Figure 1D). In contrast, after neuromuscular blockade there were, on average, 10.9 ± 1.1 tSC sprouts per NMJ after 5 days of immobilization, a level that was maintained at 8 days of immobilization (10.3 ± 0.9 per NMJ; $P < 0.001$, one-way ANOVA with Tukey post hoc vs. control: $P < 0.001$ for 5 and 8 days immobilized animals). Motor axon terminals also displayed a considerable increase in the number of sprouts at the neuromuscular synapse (Figure 1E). While there were only 0.2 ± 0.1 axonal sprouts per control NMJ, their numbers rose to 3.2 ± 0.4 per NMJ at 5 days of immobilization and the numbers continued to climb until the experimental endpoint at 8 days immobilization (6.3 ± 0.9 per NMJ; $P < 0.001$, one-way ANOVA with Tukey post hoc vs. control: $P < 0.001$ for 5 and 8 days immobilized animals). Nonetheless, the number of axon terminal sprouts did not approach that of tSCs. This observed lag in the time-course of increase in the number of axon terminal sprout compared with those of tSCs mirrors the relationship between the two concerning the fraction of NMJs that produced sprouts. It is likely that axonal response to lack of neuromuscular synaptic transmission and the resulting depolarization of the muscle fibre follows and is dependent on the response of the associated tSCs. This idea is consistent with previous observations from partially denervated muscles in which tSC processes guide axonal sprouts towards nearby denervated endplates.¹¹

Synaptic basal lamina

The synaptic localization of the two synaptic basal lamina proteins, agrin and laminin $\beta 2$ subunit, remained unaltered at 5 days post immobilization (Figure 2), a time-point at which robust sprouting activity was undertaken by both motor axon terminals and tSCs. The localization to NMJs a third synaptic basal lamina component, acetylcholinesterase, also faithfully mirrored that of the postsynaptic AChRs just as in control animals (Figure S3). The neuromuscular synaptic basal lamina appeared stable and, therefore, was unlikely to contain molecular agents responsible for driving the observed morphological alterations.

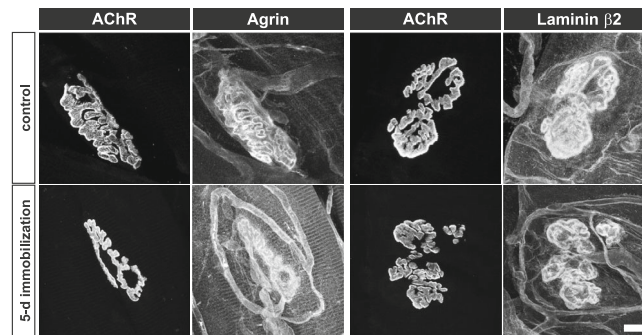


Figure 2 Synaptic basal lamina components remain localized to NMJs after pharmacological postsynaptic blockade. Agrin and laminin $\beta 2$ —two components of synaptic basal lamina responsible for differentiation and maintenance of pre- and post-synaptic specializations at NMJs, respectively—remain highly concentrated at NMJs. In addition to their distributions that mirror the AChR aggregation within the post-synaptic muscle membrane, each is found labeling SC endoneurium, as well as the capillaries.

Direct electrical stimulation of skeletal muscle dampens sprouting activity

The direct unilateral electrical stimulation of the soleus muscle had no apparent effect on the changes postsynaptic AChR assembly undergoes subsequent to the α -cobratoxin-mediated blockade. The number of discrete AChR-rich islands and endplate area of NMJs in soleus of stimulated animals remained suppressed compared with control animals and did not differ from those of non-stimulated 5 and 8 days immobilized animals (Figure 3B,C). This inability of muscle stimulation to reverse the effect of pharmacological denervation on the postsynaptic assembly at the NMJ was surprising given the restoration of muscle fibre cross sectional area in animals that had been subjected to postsynaptic neuromuscular blockade for 5 days (Figure S4). This apparent disconnect between muscle cross-sectional area and endplate size, may be explained by the removal of postsynaptic AChRs that had been rendered inactive by α -cobrotoxin from the surface of muscle fibres made electrically active by direct stimulation.¹²

Chronic electrical stimulation of soleus did not reduce the fraction of NMJs that produced sprouts, glial, or axonal (Figure S5) in absence of cholinergic synaptic transmission to postsynaptic muscle fibres. It did, however, impact the number of sprouts the tSCs and axon terminals produced (Figure 3D,E). Within muscles stimulated for 8 days concurrent with immobilization, tSCs produced on average 6.7 ± 0.5 sprouts per NMJ compared with 10.3 ± 0.9 per NMJ ($P < 0.001$) in unstimulated muscles from rats immobilized also for 8 days (Figure 3D). Surprisingly, chronic electrical stimulation similarly reduced the number of tSC sprouts in the contralateral, non-stimulated soleus muscles of the same rats (6.9 ± 0.5 per NMJ, $P < 0.001$). The dampened tSC sprouting response was evident also in animals stimulated during the first 5 days of immobilization, in both stimulated and non-stimulated contralateral soleus muscles

(7.6 ± 0.6 and 6.4 ± 0.5 per NMJ, respectively vs. 10.9 ± 1.1 in 5 days unstimulated soleus; $P < 0.01$ – 0.001). In addition, the number of synaptic glial sprouts did not differ between muscles stimulated for 5 and 8 days (7.6 ± 0.6 vs. 6.7 ± 0.5) but remained significantly greater than in control, non-immobilized animals (0.9 ± 0.2 per NMJ, $P < 0.001$). While the number of axonal sprouts in soleus muscles subjected to direct stimulation (Figure 3E) remained elevated both after 5 and 8 days immobilization (2.0 ± 0.4 and 3.2 ± 0.5 , respectively, vs. 0.2 ± 0.1 control; $P < 0.001$), there was, nonetheless, (i) a significant reduction compared with non-stimulated immobilized rat motor axon terminals (5 days: 2.0 ± 0.4 vs. 3.2 ± 0.4 , $P < 0.05$; 8 days: 3.2 ± 0.5 vs. 6.3 ± 0.9 ; $P < 0.001$) and (ii) the non-stimulated soleus muscles on the contralateral side in both 5 and 8 days stimulated immobilized rats showed similar reductions in the number of axon terminal sprouts to their electrically stimulated counterparts (5 days: 1.7 ± 0.3 vs. 2.0 ± 0.4 ; 8 days: 3.4 ± 0.5 vs. 3.2 ± 0.5). The chronic electrical stimulation of muscles in pharmacologically denervated rats, thus, dampened and/or slowed the sprouting responses of both tSCs and motor axon terminals in both stimulated and unstimulated contralateral soleus muscles, that is, an inhibitory effect most likely mediated through an activity-dependent muscle-derived soluble factor.

NMJ-associated differentially expressed genes (DEGs)

According to differential expression analysis, a total of 4913 DEGs were identified in the soleus after 8 days pharmacological denervation compared with sham-operated controls ('D8 vs. D0'). In rats exposed to pharmacological denervation and unilateral direct electrical stimulation of the soleus for 8 days, a total of 2163 and 1419 DEGs were identified in the stimulated and unstimulated contralateral soleus, respectively,

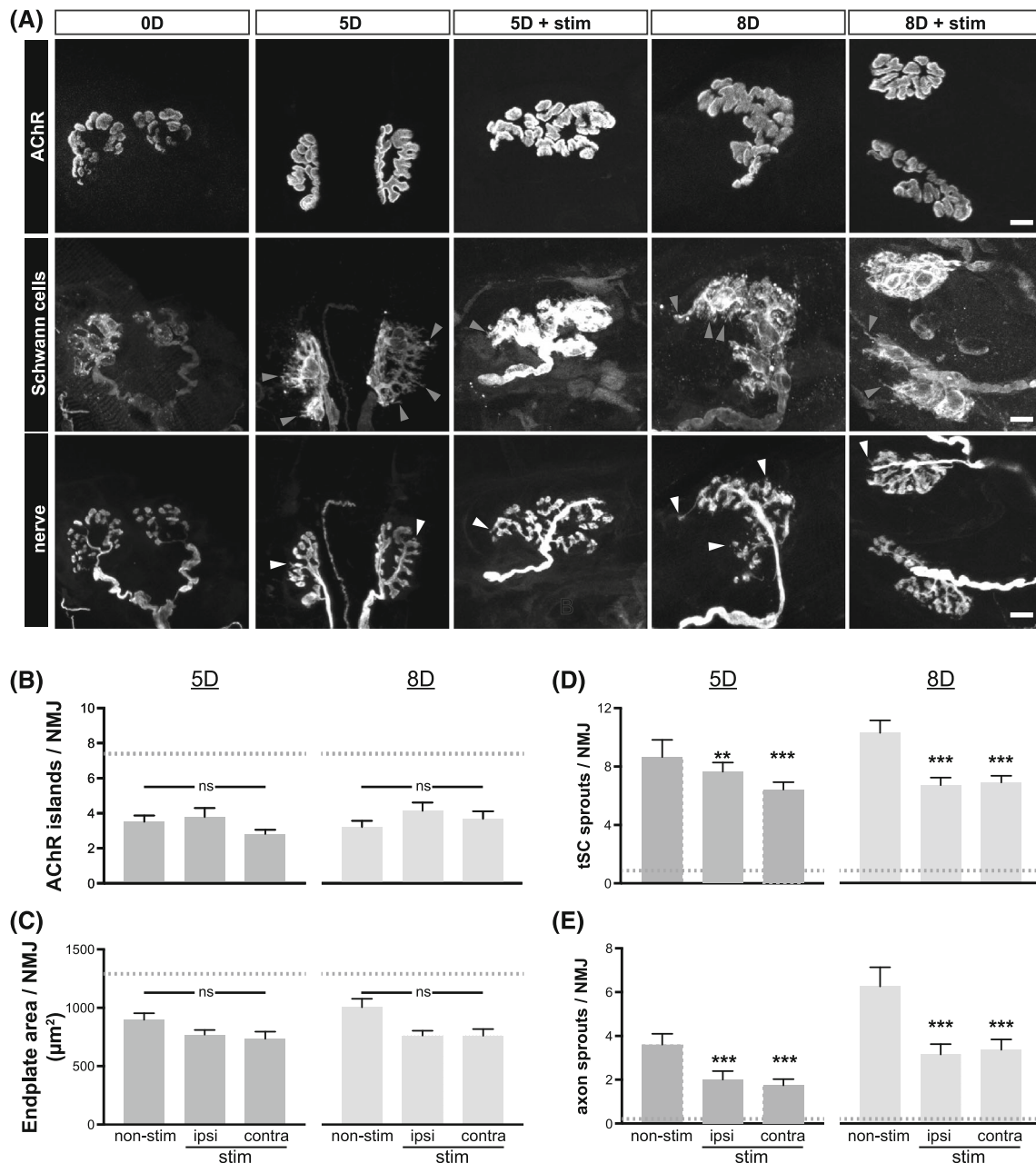


Figure 3 Electrical stimulation dampens the sprouting responses to pharmacological silencing of neuromuscular synaptic transmission. (A) Top row: Postsynaptic AChR aggregates from control as well as 5 and 8 days immobilized rats with or without direct electrical stimulation to the right soleus muscle. Second and third rows: Disposition of tSCs (second row) and motor axon terminals (third row) at NMJs of soleus muscles from control, non-immobilized, and 5 and 8 days immobilized rats with or without direct electrical stimulation. Scale bars = 10 μ m. (B) The number of distinct AChR-rich islands per NMJ in electrically stimulated soleus muscle and the non-stimulated contralateral soleus muscles is compared with NMJs of soleus muscles from non-stimulated rats. No change is observed at either of the time points examined (5 and 8 days of α -cobrotoxin-induced synaptic blockade). Grey dashed line indicates the control values without synaptic blockade. (C) The endplate area of electrically stimulated soleus muscle and the non-stimulated contralateral soleus muscles is compared with NMJs of soleus muscles from non-stimulated rats. No change is observed at either of the time points examined (5 and 8 days of α -cobra toxin-induced synaptic blockade). (D) The number of synaptic SC sprouts was significantly reduced in 8 days immobilized rats that had also received muscle stimulation compared with those that did not. The reduction in SC sprouting response was seen in the soleus muscle that received the direct electrical stimulation as well as the unstimulated contralateral soleus muscle of the same rats. (E) Direct electrical stimulation of soleus muscles reduces the number of motor axon terminal sprouts in both 5 and 8 days immobilized rats. This reduction in the number of terminal sprouts was observed in both stimulated and contralateral, unstimulated soleus muscles. In all experimental conditions, the number of axonal and SC sprouts remain elevated vs. the control, non-immobilized rats (grey dashed lines). One-way ANOVA, Tukey post-hoc analysis: *** $P < 0.001$, ** $P < 0.01$ vs. non-stimulated control samples at either 5 or 8 days immobilized cohorts.

compared with the soleus in rats exposed to 8 days pharmacological denervation without electrical stimulation (comparisons 'D8ES vs. D8' and 'D8ESCL vs. D8').

According to enrichment analysis, there were several GO terms related to neuromuscular junction structure and functions, such as 'neuromuscular junction', 'postsynaptic cytoskeleton', 'axonal transport of mitochondrion', 'receptor localization to synapse', 'neurotransmitter metabolic process', 'axonal growth cone', 'neurotrophin receptor binding', and 'presynaptic membrane' (Figure 4A). Most of these GO terms had strong negative z-scores when comparing D8 and D0, that is, involved DEGs and relevant biofunctions were down-regulated in response to 8 days pharmacological denervation. In the comparisons 'D8ES vs. D8' and 'D8ESCL vs. D8', enriched GO terms showed positive z-scores, suggesting a restoring effect of electrical stimulation on these biofunctions in both stimulated and unstimulated soleus. The restoring effect was confirmed by the detailed fold change information of involved DEGs, such as the term 'neuromuscular junction', and multiple DEGs induced by 8 days pharmacological denervation showed opposite fold change direction in response to electrical stimulation on both stimulated and unstimulated sides (Figure 4B, S6).

A total of 244 DEGs were involved in the enriched GO terms (Table S1). Specifically, 195 DEGs were identified when comparing 'D8 vs. D0', contributing to disarrangements in neuromuscular junction induced by long-term post-synaptic neuromuscular transmission blockade. In response to electrical stimulation, 94 DEGs were identified in the comparison of 'D8ES vs. D8', 65 of which were overlapped in the comparisons 'D8ES vs. D8' and 'D8 vs. D0' with the large majority showing opposite fold change directions in these two comparisons (Figure 4C,D). Thus, electrical stimulation had a restoring effect among the 65 overlapped DEGs. Furthermore, 72 DEGs were identified in the comparison of 'D8ESCL vs. D8', 41 of which overlapped with the comparisons 'D8ESCL vs. D8' and 'D8 vs. D0' with most of them showing an opposite fold change direction between these two comparisons (Figure 4C,D), indicating a restoring effect of electrical stimulation also on the unstimulated soleus. In addition, 44 DEGs overlapped between the comparisons 'D8ES vs. D8' and 'D8ESCL vs. D8' and all of them showed the same fold change direction, demonstrating similar alterations in stimulated and unstimulated soleus in response to 8 days electrical stimulation. Among all comparisons, there were 33 DEGs with both significant restoring and crossover effect of electrical stimulation (Figure 4C,E).

All 244 DEGs were subject to PPI network analysis. Thirty gene hubs with the highest betweenness/association with other genes were highlighted in the network and proposed to contribute to relevant bioprocesses (Figure 5A). Among which, eight genes exhibited the tendency of restoring and crossover effect of electrical stimulation, including *Stx1a*, *Cacna1a*, *Lamb2*, *Bdnf*, *Jun*, *Gdnf*, *Cxcr4*, and *Met* (Figure 5B).

Cytokine/chemokine expression in muscle and plasma

Skeletal muscle is a producer of cytokines/chemokines (myokines), which have autocrine, paracrine, and endocrine functions.¹³ A proximity extension assay proteomics approach was taken using a mouse cytokine/chemokine panel to explore the mechanism(s) underlying the muscle-nerve crosstalk and crossover communication. Among the 92 mouse cytokines/chemokines in this panel, 70 showed cross-reactivity with rat muscle and plasma samples (Table S2). Cytokines/chemokines were searched for demonstrating increased levels in plasma, stimulated and unstimulated soleus and being different from 8 days unstimulated rats. The cytokines *Ccl3* and *TGFβ1* fulfilled these criteria suggesting a mechanism where cytokines/chemokine production induced by electrical stimulation, released systemically, and having both paracrine and endocrine functions (Figure 6).

Discussion

The major observations from this study are as follows: (i) A tSC and axonal sprouting in response to post-synaptic blockade of neuromuscular transmission with tSCs preceding/leading axon sprouts. (ii) The frequency and the extent of sprouts correlated with the duration of postsynaptic blockade. (iii) Direct electrical stimulation of muscle slowed the progression of the sprouting response on the stimulated and contralateral unstimulated side. (iv) Gene expression analyses confirmed a cross-over effect in genes related to NMJ structure and function. These genes typically showed the opposite pattern than in control immobilized soleus muscles in the absence of electrical stimulation. (v) Results suggest an electrical stimulation induced cytokine/chemokine release with paracrine/endocrine effects on the NMJ on both the stimulated and contralateral unstimulated side.

Following partial denervation, nerve growth from remaining innervated endplates to denervated endplates represents a mechanism for maintenance of muscle function after nerve injuries. The experiments of Brown and his collaborators¹⁴ provide the generally accepted explanation of how sprouting is generated: paralysis of the NMJ achieved by block of nerve impulses reaching the nerve terminal stimulates sprouting whereas electrical stimulation of muscle inhibits it. Extension of tSC processes from the denervated NMJs that provide the 'bridges' across which axon terminals from still intact NMJs sprout.² Similarly, formation of these glial bridges between synaptic sites is inhibited by direct electrical stimulation of the muscle.¹⁵ Thus, electrical stimulation may negatively impact on the reinnervation in a clinical situation with neuromuscular blockade or motoneuron loss. Other interventions

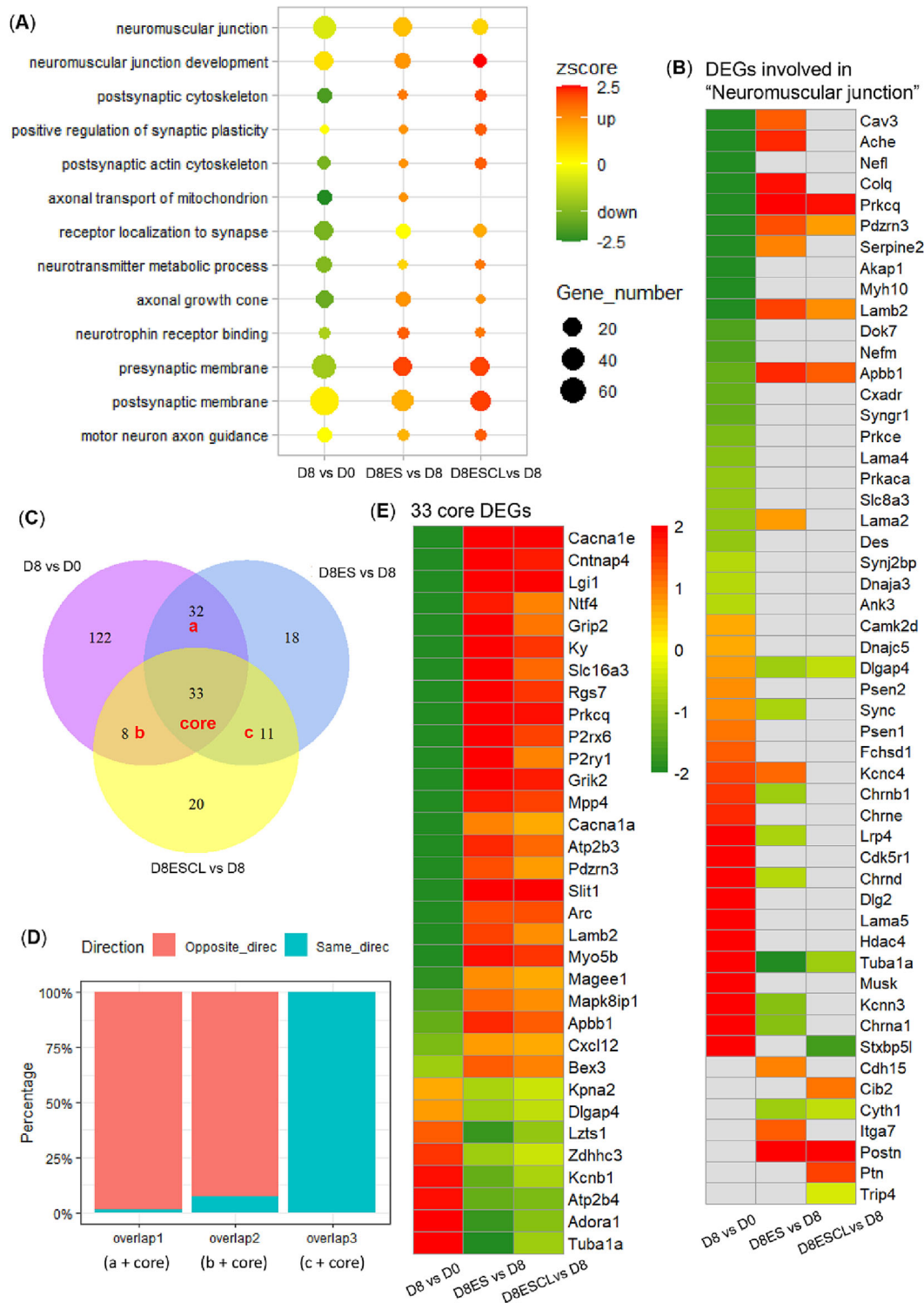


Figure 4 Differentially expressed genes related to neuromuscular junction. (A) GO terms related to neuromuscular junction enriched by DEGs in all comparisons; (B) fold change information of DEGs involved in ‘neuromuscular junction’; (C) Venn diagram of DEGs identified in each comparison. ‘a + core’ (overlap 1) represents the overlapped DEGs between ‘D8 vs. D0’ and ‘D8ES vs. D8’, ‘b + core’ (overlap 2) represents the overlapped DEGs between ‘D8 vs. D0’ and ‘D8ESCL vs. D8’, ‘c + core’ (overlap 3) represents the overlapped DEGs between ‘D8ES vs. D8’ and ‘D8ESCL vs. D8’; (D) percentage of DEGs in overlap 1–3 with same or opposite direction of fold change; (E) fold change information of 33 core DEGs overlapped among all comparisons. D0: Soleus muscle of sham-operated rats (*n* = 5); D8: Soleus muscle of 8 day pharmacological denervated rats (*n* = 5); D8ES: Electrical stimulated soleus muscle of 8 day pharmacological denervated rats with electrical stimulation (*n* = 8); D8ESCL: Unstimulated contralateral soleus muscle of 8 day pharmacological denervated rats with electrical stimulation (*n* = 8).

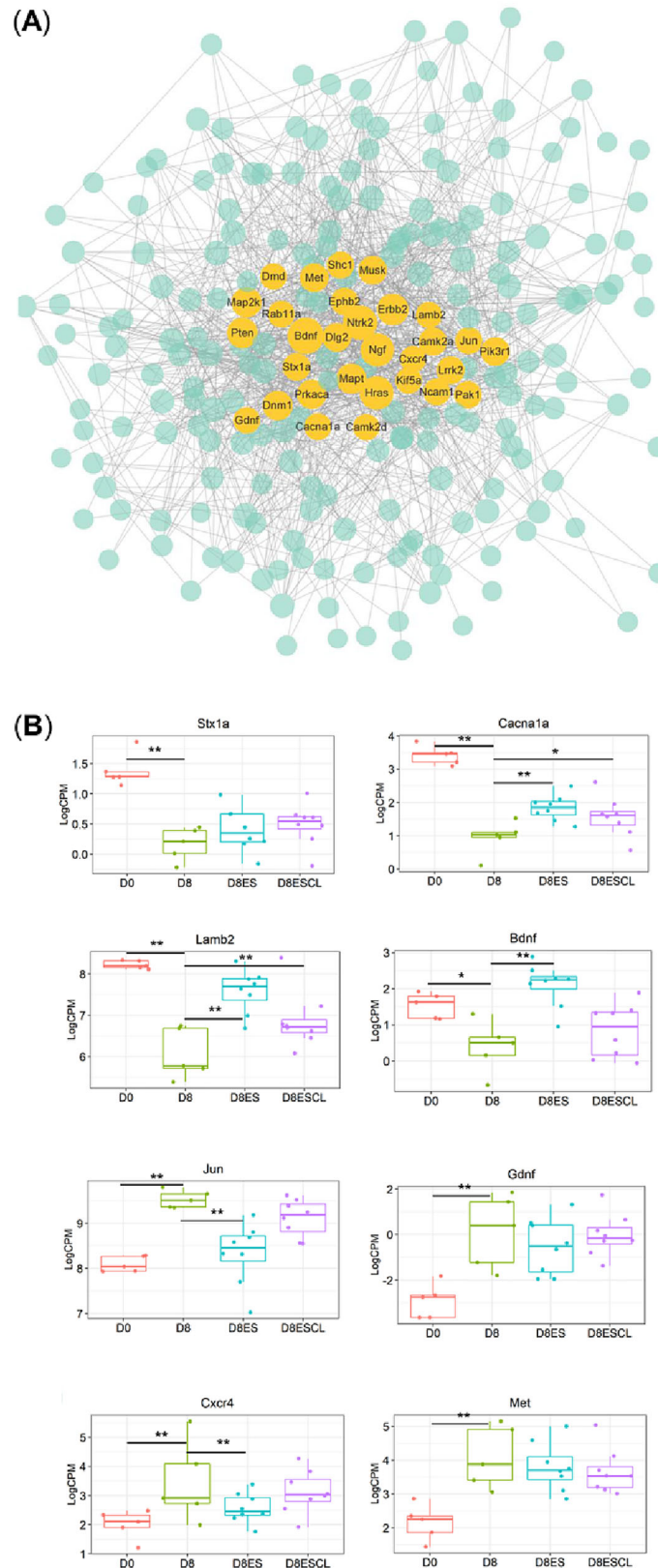


Figure 5 The PPI network constructed by 244 DEGs related to neuromuscular junction. (A) Thirty gene hubs with the strongest betweenness/association with other genes and (B) boxplot for the eight gene hubs with restoring and crossover effect of electrical stimulation. Dot size represents the betweenness/association among genes (* $P < 0.05$; ** $P < 0.01$).

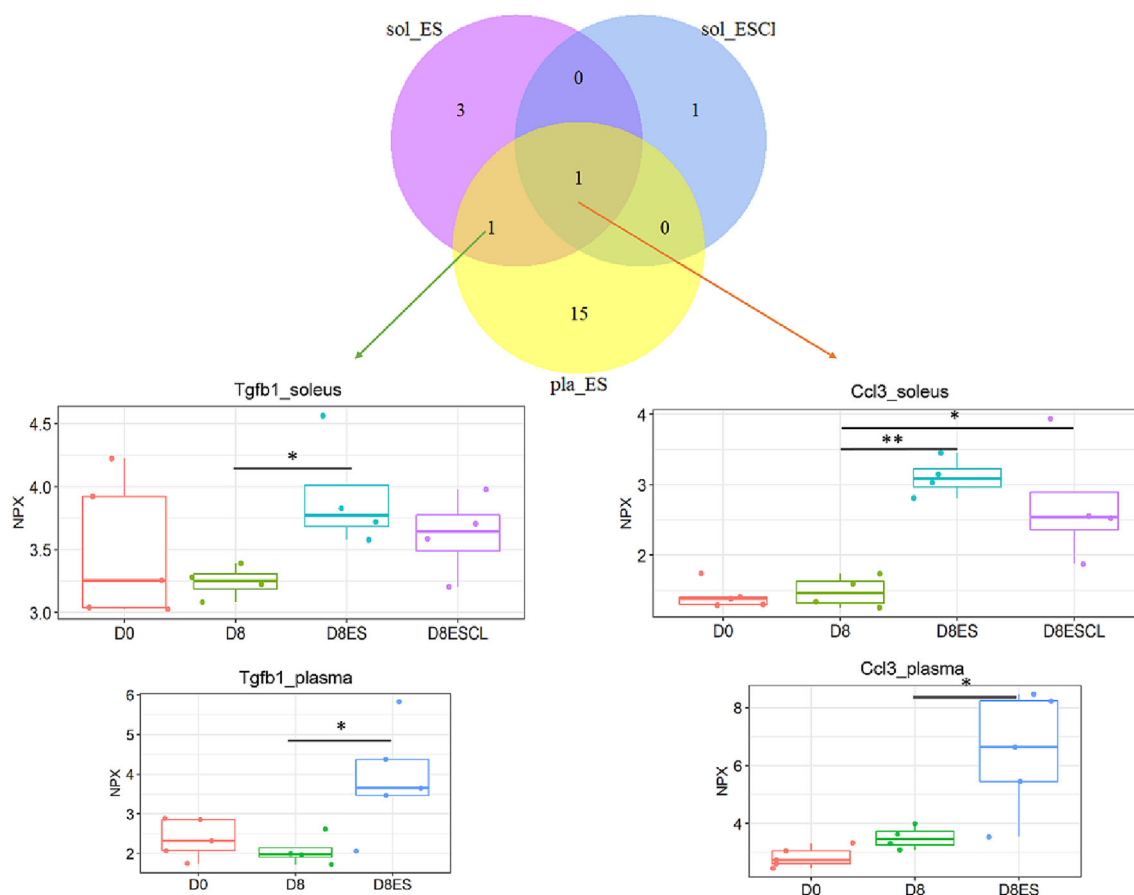


Figure 6 Identification of cytokine/chemokine in muscle and plasma mediating the crossover effect. D0: Soleus muscle of sham-operated rats ($n = 5$); D8: Soleus muscle of 8 day pharmacological denervated rats ($n = 4$); D8ES: Electrical stimulated soleus muscle of 8 day pharmacological denervated rats with electrical stimulation ($n = 5$); D8ESCL: Unstimulated contralateral soleus muscle of 8 day pharmacological denervated rats with electrical stimulation ($n = 5$).

targeting muscle wasting such as passive mechanical loading may prove advantageous compared with electrical stimulation and is currently being studied in the experimental model.

Our experiments depart from the experiments done to date in that the paralysis of the muscle is achieved by systemic application of α -cobrotoxin that blocks the AChR. The remarkable result is that, while sprouting of both nerves and tSCs occurs, this sprouting is much less extensive than that achieved by physical denervation or paralysis of the muscle nerve. Thus, blocking the release of ACh from the muscle innervation is much more effective in eliciting sprouting than is postsynaptic blockade of the action of the ACh on the receptors in the muscle fibre. This raises the issue of what the most proximate cause of sprouting is in the case of muscle denervation and block of nerve conduction. tSC response to different modes of synaptic silencing potentially help reconcile the different responses. tSCs possess the means to sense presynaptic activity: muscarinic AChRs and purinergic receptors sense ACh and ATP released from the presynaptic nerve terminals.¹⁶ tSCs, thus, possess the means to differentiate and potentially produce distinct responses to pre- and post-

synaptic. In case of the physical denervation, the tSCs in absence of motor axon—and its trophic support—engage in up-regulated autocrine neuregulin signalling.¹⁷ Activation of tSCs by neuregulin—either soluble or tethered to motor axon membrane—produces morphological alterations at NMJs.¹⁸ It is, however, presently unclear whether the responses to these stimuli are additive.

To identify potential cellular/molecular correlates of the sprouting events observed at NMJs in response to pharmacological denervation with an intact motoneuron, we examined the distribution of two synaptic basal lamina components whose absence have been associated with axonal or glial process outgrowth: agrin and laminin $\beta 2$ subunit. However, the NMJ synaptic basal lamina appeared stable and unaltered overall in response to the postsynaptic blockade of neuromuscular transmission and, therefore, was unlikely to contain molecular agents responsible for driving the observed morphological alterations. Irrespective of the upstream cue that produces morphological changes of the synapse, a potential downstream effector for postsynaptic changes is MuRF1. A previous study has implicated its activity in regulating

stability and turnover of AChR in muscle fibres subjected to atrophy-inducing conditions.¹⁹ It will be of interest to further examine in the future whether the yet-unidentified myokine and MuRF1 reside in the same molecular pathway that regulate postsynaptic size and stability in response to changes in skeletal muscle activity.

The tSCs possess distinct classes of AChRs (metabotropic and muscarinic) that respond to ACh molecules than those present on the postsynaptic muscle fibre (ionotropic and nicotinic). tSCs sprouts are known to have powerful effects on nerve growth by guiding the growth of nerve processes^{2,3} and may be the primary force driving and guiding the sprouting process we presently report. Thus, ACh release in rats exposed to post-synaptic neuromuscular blockade may act directly on tSC AChRs to reduce sprouting compared with peripheral denervation or paralysis of the muscle nerve. However, this appears an unlikely mechanism underlying the cross-over effect on NMJ sprouting on the contralateral unstimulated muscle.

To our knowledge, there is only one previous publication where a cross-over effect of electrical stimulation has been reported. More than four decades ago, O'Brien and co-workers reported a more rapid elimination of polyneuronal innervation in developing rat soleus muscle on both stimulated and unstimulated side in response to unilateral electrical stimulation of the sciatic nerve.²⁰ This cross-over effect was interpreted to be due to reflex activation via the crossed-extensor reflex and the release of agents from the stimulated and reflex activated muscle acting on the NMJ.²⁰ This was in part supported by the activation of muscles on the contralateral side of the electrical stimulation. In this study, this is an unlikely mechanism underlying the cross-over effect because muscles were pharmacologically paralysed, and a muscle contraction was only observed in the directly stimulated distal hindlimb muscle. An axonal retrograde transport from the stimulated soleus via the spinal cord or via an altered sympathetic influence on the NMJ²¹ cannot be completely ruled out as a mechanism underlying the cross-over effect and need to be addressed further.

RNAseq enrichment analyses suggest potential disarrangement and downregulation of NMJ structure and function in response to long-term post-synaptic blockade of neuromuscular transmission. However, these changes were partially restored in response to direct muscle electrical stimulation. A similar restoring effect was observed in the unstimulated contralateral soleus supporting a crosstalk between stimulated and unstimulated muscle. Among NMJ related DEGs, 33 were significantly altered by the 8 day pharmacological denervation and restored by electrical stimulation on both the stimulated and unstimulated soleus muscle. Some of the down-regulated DEGs in the D8 controls groups were upregulated in response to electrical stimulation, that is, genes involved in the regulation of voltage-gated potassium

channels, neuronal growth regulation and cell survival (Lgi1),²² muscle innervation and NMJ differentiation (Ntf4),²³ NMJ function, maturation and stabilization (Ky),²⁴ regulation of nerve homeostasis (P2rx6),²⁵ regulation of MuSK signalling (Pdzm3), motor axon guidance and extension (Slit1),²⁶ neuron outgrowth, cell adhesion and signalling (Lamb2),²⁷ regulation of axonal growth and growth (Mapk8ip1),²⁸ and NMJ formation (Apbb1).²⁹ The decreased expression of these genes confirms the dysfunctions of NMJ in response to post-synaptic blockade of neuromuscular transmission and the restoring effect of electrical stimulation.

Protein–protein network analyses identified several hub genes with important biological processes related to the NMJ. Some of these hub genes were downregulated by 8 day pharmacological denervation and upregulated by electrical stimulation. For example, Strx1a (syntaxin-1A),³⁰ a member of syntaxins, playing an essential role in calcium-dependent exocytosis and endocytosis of hormone and neurotransmitter and, thus, of importance for proper NMJ synaptic function. Voltage-dependent P/Q-type calcium channels (Cacna1a), involved in multiple calcium-dependent processes, such as neurotransmitter release.³¹ Lamb2, a laminin subunit and synaptic space protein expressed at the NMJ.²⁷ Bdnf, enhances motoneuron survival, growth and is implicated in both formation and maturation of NMJs.³² Given the importance of these hub genes, these results support the negative impact of post-synaptic neuromuscular blockade on the NMJ and the restoring effect of direct muscle stimulation on the NMJ of both the stimulated and unstimulated soleus.

Some hub genes upregulated by 8 day pharmacological denervation were modestly downregulated by electrical stimulation such as, c-Jun, Gdnf, Cxcr4, and c-MET. c-Jun has been reported to play a role in neuronal sprouting.³³ Exogenous expression of c-Jun induces neurite extension in a neuronal-like cell line.³⁴ Gdnf, glial cell line-derived neurotrophic factor, is expressed at high levels in Schwann cells to induce neurite sprouting in axonal injury models.³⁵ Cxcr4, a component of the CXC12a-CXCR4 axis, plays an important role in the regeneration of the NMJ after motor axon injury and in axonal elongation/branching.³⁶ Met, or c-MET, promotes axonal growth via HGF/c-Met signalling under the regulation of TGF- β .³⁷

Muscle cells communicate with other cells by cytokine/chemokine (myokine) production having autocrine, paracrine and endocrine effects.³⁸ The increased expression of Ccl3 and TGF β 1 in plasma and in both stimulated and unstimulated soleus but not in control 8 day pharmacologically paralysed and ventilated rats support a crosstalk from stimulated to unstimulated muscles via systemic release of myokines. Although the role of Ccl3 (aka MCP-1 α) and TGF β 1 in reducing Schwann cell and axon outgrowth in response to direct electrical muscle stimulation remains unknown it is interesting to note that both these

cytokines/chemokines have been reported in neuromuscular junction pathology. Ccl3 being involved in the intrinsic neuromuscular control of the colon, Wallerian degeneration, and pathological adaptive responses of Schwann cells.³⁹ Furthermore, TGF β 1 inhibits the fibroblast growth factor binding protein 1 (FGFBP1) which enhances the biological activity of FGF-1 and FGF-2, both implicated in axonal regeneration.⁴⁰ However, more than 650 myokines have been identified in skeletal muscle and only a small fraction of them were detected with the exploratory cytokine/chemokine panel used in this study, but most importantly, the results from these analyses demonstrate a potential mechanism underlying the cross-over effect. Alternatively, cell-to-cell communication via intercellular transfer of microvesicles/exosomes containing a variety of biological materials (mRNAs, miRNAs, proteins, and lipids) may directly target cells or transfer surface receptors with effects on distant muscles. Exosomes derived from myocytes are able to regulate metabolic activity and triggered by increased intracellular Ca²⁺ levels, such as in response to direct muscle stimulation.⁴¹ Thus, microvesicles/exosomes released in response to direct muscle stimulation may induce the release of microvesicles/exosomes carrying information affecting both nearby and distant NMJs and muscle cells.

References

- Li Y, Thompson WJ. Nerve terminal growth remodels neuromuscular synapses in mice following regeneration of the postsynaptic muscle fiber. *J Neurosci* 2011;**31**: 13191–13203.
- Son Y-J, Thompson WJ. Nerve sprouting in muscle is induced and guided by processes extended by Schwann cells. *Neuron* 1995;**14**:133–141.
- Son Y-J, Thompson WJ. Schwann cell processes guide regeneration of peripheral axons. *Neuron* 1995;**14**:125–132.
- Love FM, Son YJ, Thompson WJ. Activity alters muscle reinnervation and terminal sprouting by reducing the number of Schwann cell pathways that grow to link synaptic sites. *J Neurobiol* 2003;**54**: 566–576.
- Brown MC, Holland RL, Hopkins WG, Keynes RJ. An assessment of the spread of the signal for terminal sprouting within and between muscles. *Brain Res* 1981;**210**:145–151.
- Herridge MS. Recovery and long-term outcome in acute respiratory distress syndrome. *Crit Care Clin* 2011;**27**:685–704.
- Parry SM, Berney S, Granger CL, Koopman R, El-Ansary D, Denehy L. Electrical muscle stimulation in the intensive care setting: a systematic review. *Crit Care Med* 2013;**41**: 2406–2418.
- Mohan SK, Yu C. Structure function relationship of cobrotoxin from *NAJA NAJA ATRA*. *Toxin Rev* 2007;**26**:99–122.
- Ballice-Gordon RJ, Breedlove SM, Bernstein S, Lichtman JW. Neuromuscular junctions shrink and expand as muscle fiber size is manipulated: in vivo observations in the androgen-sensitive bulbocavernosus muscle of mice. *J Neurosci* 1990;**10**:2660–2671.
- Rich MM, Pinter MJ. Sodium channel inactivation in an animal model of acute quadriplegic myopathy. *Ann Neurol* 2001;**50**: 26–33.
- Kang H, Tian L, Mikesh M, Lichtman JW, Thompson WJ. Terminal Schwann cells participate in neuromuscular synapse remodeling during reinnervation following nerve injury. *J Neurosci* 2014;**34**: 6323–6333.
- Ballice-Gordon RJ, Lichtman JW. Long-term synapse loss induced by focal blockade of postsynaptic receptors. *Nature* 1994;**372**: 519–524.
- Severinsen MCK, Pedersen BK. Muscle-organ crosstalk: the emerging roles of myokines. *Endocr Rev* 2020;**41**:594–609.
- Brown MC, Holland RL, Hopkins WG. Motor nerve sprouting. *Ann Rev Neurosci* 1981;**4**:17–42.
- Love FM, Thompson WJ. Glial cells promote muscle reinnervation by responding to activity-dependent postsynaptic signals. *J Neurosci* 1999;**19**:10390–10396.
- Rousse I, St-Amour A, Darabid H, Robitaille R. Synapse-glia interactions are governed by synaptic and intrinsic glial properties. *Neuroscience* 2010;**167**:621–632.
- Carroll SL, Miller ML, Frohnert PW, Kim SS, Corbett JA. Expression of neuregulins and their putative receptors, ErbB2 and ErbB3, is induced during Wallerian degeneration. *J Neurosci* 1997;**17**:1642–1659.
- Lee YI, Li Y, Mikesh M, Smith I, Nave KA, Schwab MH, et al. Neuregulin1 displayed on motor axons regulates terminal Schwann cell-mediated synapse elimination at developing neuromuscular junctions. *Proc Natl Acad Sci U S A* 2016;**113**:E479–E487.
- Rudolf R, Bogomolovas J, Strack S, Choi KR, Khan MM, Wagner A, et al. Regulation of nicotinic acetylcholine receptor turnover by MuRF1 connects muscle activity to endo/lysosomal and atrophy pathways. *Age* 2013;**35**:1663–1674.
- O'Brien RA, Ostberg AJ, Vrbova G. Observations on the elimination of polyneuronal innervation in developing mammalian skeletal muscle. *J Physiol* 1978;**282**: 571–582.
- Khan MM, Lustrino D, Silveira WA, Wild F, Straka T, Issop Y, et al. Sympathetic innervation controls homeostasis of neuromuscular junctions in health and disease. *Proc Natl Acad Sci U S A* 2016;**113**:746–750.
- Fukata Y, Adesnik H, Iwanaga T, Bredt DS, Nicoll RA, Fukata M. Epilepsy-related ligand/receptor complex LGI1 and ADAM22 regulate synaptic transmission. *Science* 2006;**313**:1792–1795.
- Stemple JC, Andreatta RD, Seward TS, Angadi V, Dietrich M, McMullen CA.

Funding

This work was supported by NINDS Grant NS20480 to W.T. and Y.L. and by grants from the Swedish Research Council (8651), the Erling-Persson Foundation, Stockholm City Council (Alf 20150423 and 20170133), CIF, and Karolinska Institutet to L.L.

The study conforms with the ethical guidelines of the *Journal of Cachexia, Sarcopenia and Muscle*⁴² and were approved by ethical committees at Uppsala University and Karolinska Institutet.

Conflict of interest

The authors declare no financial or nonfinancial competing interests.

Online supplementary material

Additional supporting information may be found online in the Supporting Information section at the end of the article.

- Enhancement of aging rat laryngeal muscles with endogenous growth factor treatment. *Physiol Rep* 2016;**4**:e12798.
24. Blanco G, Coulton GR, Biggin A, Grainge C, Moss J, Barrett M, et al. The kyphoscoliosis (ky) mouse is deficient in hypertrophic responses and is caused by a mutation in a novel muscle-specific protein. *Hum Mol Genet* 2001;**10**:9–16.
25. Patrilli-Cram J, Coover RA, Jankowski MP, Ratner N. Purinergic signaling in peripheral nervous system glial cells. *Glia* 2021;**69**:1837–1851.
26. Ringstedt T, Braisted JE, Brose K, Kidd T, Goodman C, Tessier-Lavigne M, et al. Slit inhibition of retinal axon growth and its role in retinal axon pathfinding and innervation patterns in the diencephalon. *J Neurosci* 2000;**20**:4983–4991.
27. Nishimune H, Sanes JR, Carlson SS. A synaptic laminin-calcium channel interaction organizes active zones in motor nerve terminals. *Nature* 2004;**432**:580–587.
28. Dajas-Bailador F, Jones EV, Whitmarsh AJ. The JIP1 scaffold protein regulates axonal development in cortical neurons. *Curr Biol* 2008;**18**:221–226.
29. Streckler P, Ludewig S, Rust M, Mundinger TA, Gorlich A, Krachan EG, et al. FE65 and FE65L1 share common synaptic functions and genetically interact with the APP family in neuromuscular junction formation. *Sci Rep* 2016;**6**:25652.
30. Craig TJ, Anderson D, Evans AJ, Girach F, Henley JM. SUMOylation of syntaxin1A regulates presynaptic endocytosis. *Sci Rep* 2015;**5**:17669.
31. Kozminski W, Pera J. Involvement of the peripheral nervous system in episodic ataxias. *Biomedicine* 2020;**8**:448.
32. Je HS, Yang F, Ji YY, Potluri S, Fu XQ, Luo ZG, et al. ProBDNF and mature BDNF as punishment and reward signals for synapse elimination at mouse neuromuscular junctions. *J Neurosci* 2013;**33**:9957–9962.
33. Barnat M, Enslin H, Propst F, Davis RJ, Soares S, Nothias F. Distinct roles of c-Jun N-terminal kinase isoforms in neurite initiation and elongation during axonal regeneration. *J Neurosci* 2010;**30**:7804–7816.
34. Dragunow M, Xu R, Walton M, Woodgate A, Lawlor P, MacGibbon GA, et al. c-Jun promotes neurite outgrowth and survival in PC12 cells. *Brain Res Mol Brain Res* 2000;**83**:20–33.
35. Stanga S, Boido M, Kienlen-Campard P. How to build and to protect the neuromuscular junction: the role of the glial cell line-derived neurotrophic factor. *Int J Mol Sci* 2000;**22**:136.
36. Zanetti G, Negro S, Megighian A, Mattarei A, Lista F, Fillo S, et al. A CXCR4 receptor agonist strongly stimulates axonal regeneration after damage. *Ann Clin Transl Neurol* 2019;**6**:2395–2402.
37. Desole C, Gallo S, Vitacolonna A, Montarolo F, Bertolotto A, Vivien D, et al. HGF and MET: from brain development to neurological disorders. *Front Cell Dev Biol* 2021;**9**:683609.
38. Severinsen MCK, Pedersen BK. Muscle-organ crosstalk: the emerging roles of myokines (vol 41, pg 594, 2020). *Endocr Rev* 2021;**42**:97–99.
39. White AR, Holmes GM. Anatomical and functional changes to the colonic neuromuscular compartment after experimental spinal cord injury. *J Neurotrauma* 2018;**35**:1079–1090.
40. Taetzsch T, Tenga MJ, Valdez G. Muscle fibers secrete FGFBP1 to slow degeneration of neuromuscular synapses during aging and progression of ALS. *J Neurosci* 2017;**37**:70–82.
41. Savina A, Furlan M, Vidal M, Colombo MI. Exosome release is regulated by a calcium-dependent mechanism in K562 cells. *J Biol Chem* 2003;**278**:20083–20090.
42. von Haehling S, Morley JE, Coats AJS, Anker SD. Ethical guidelines for publishing in the Journal of Cachexia, Sarcopenia and Muscle: update 2021. *J Cachexia Sarcopenia Muscle* 2021;**12**:2259–2261.